ARTHRITIS & RHEUMATISM
Vol. 60, No. 10, October 2009, pp 2902–2912
DOI 10.1002/art.24814

Thrombin-Activatable Carboxypeptidase B Cleavage of Osteopontin Regulates Neutrophil Survival and Synoviocyte Binding in Rheumatoid Arthritis

Shadi A. Sharif,[1] Xiaoyan Du,[1] Timothy Myles,[1] Jason J. Song,[2] Elizabeth Price,[1] David M. Lee,[3] Stuart B. Goodman,[1] Mariko Nagashima,[4] John Morser,[4] William H. Robinson,[2] and Lawrence L. K. Leung[2]

Objective. **Osteopontin (OPN) is a proinflammatory cytokine that plays an important role in the pathogenesis of rheumatoid arthritis (RA). OPN can be cleaved by thrombin, resulting in OPN-R and exposing the cryptic C-terminal $\alpha 4\beta 1$ and $\alpha 9\beta 1$ integrin–binding motif (SVVYGLR). Thrombin-activatable carboxypeptidase B (CPB), also called thrombin-activatable fibrinolysis inhibitor, removes the C-terminal arginine from OPN-R, generating OPN-L and abrogating its enhanced cell binding. We undertook this study to investigate the roles of OPN-R and OPN-L in synoviocyte adhesion, which contributes to the formation of invasive pannus, and in neutrophil survival, which affects inflammatory infiltrates in RA.**

Methods. **Using specifically developed enzyme-linked immunosorbent assays, we tested the synovial fluid of patients with RA, osteoarthritis (OA), and psoriatic arthritis (PsA) to determine OPN-R, OPN-L, and full-length OPN (OPN-FL) levels.**

Results. **Elevated levels of OPN-R and OPN-L were found in synovial fluid samples from RA patients, but not in samples from OA or PsA patients. Increased levels of OPN-R and OPN-L correlated with increased levels of multiple inflammatory cytokines, including tumor necrosis factor α and interleukin-6. Immunohistochemical analyses revealed robust expression of OPN-FL, but only minimal expression of OPN-R, in RA synovium, suggesting that cleaved OPN is released into synovial fluid. In cellular assays, OPN-FL, and to a lesser extent OPN-R and OPN-L, had an antiapoptotic effect on neutrophils. OPN-R augmented RA fibroblast-like synoviocyte binding mediated by SVVYGLR binding to $\alpha 4\beta 1$, whereas OPN-L did not.**

Conclusion. **Thrombin activation of OPN (resulting in OPN-R) and its subsequent inactivation by thrombin-activatable CPB (generating OPN-L) occurs locally within inflamed joints in RA. Our data suggest that thrombin-activatable CPB plays a central homeostatic role in RA by regulating neutrophil viability and reducing synoviocyte adhesion.**

Rheumatoid arthritis (RA) is a chronic, disabling systemic inflammatory joint disease, characterized by the propagation of inflammatory cells within the joint space, leading to the invasive growth of synovial tissue and the destruction of cartilage and bone (1). Recent evidence suggests that osteopontin (OPN) may play an important role in RA pathogenesis (2–4). OPN is a glycosylated phosphoprotein that functions either as a plasma proinflammatory cytokine or as an extracellular

Dr. Song is recipient of an American College of Rheumatology Research and Education Foundation Physician Scientist Development award. Dr Robinson's work was supported by NIH contract N01-HV-28183 from the National Heart, Lung, and Blood Institute. Dr. Leung's work was supported by NIH grant R01-HL-57530.

[1]Shadi A. Sharif, MS, Xiaoyan Du, PhD, Timothy Myles, PhD, Elizabeth Price, MD, Stuart B. Goodman, MD, PhD: Stanford University School of Medicine, Stanford, California; [2]Jason J. Song, MD, William H. Robinson, MD, PhD, Lawrence L. K. Leung, MD: Stanford University School of Medicine, Stanford, California, and VA Palo Alto Health Care System, Palo Alto, California; [3]David M. Lee, MD, PhD: Brigham and Women's Hospital, Boston, Massachusetts; [4]Mariko Nagashima, PhD, John Morser, PhD: Berlex Biosciences, Richmond, California.

Dr. Lee has received consulting fees, speaking fees, and/or honoraria from Resolvyx, UCB Pharma, Novartis, and Johnson & Johnson (less than $10,000 each) and from Synovex (more than $10,000); owns stock or stock options in Synovex; receives licensing fees for cadherin 11; and has received research support from MedImmune, Biogen, and Genentech.

Address correspondence and reprint requests to Lawrence L. K. Leung, MD, Division of Hematology, Stanford University School of Medicine, 269 Campus Drive, CCSR Room 1155, Stanford, CA 94305. E-mail: lawrence.leung@stanford.edu.

Submitted for publication January 30, 2009; accepted in revised form June 15, 2009.

matrix protein in bone remodeling (5,6). OPN is expressed by many different cell types, including activated immune cells such as macrophages, natural killer cells, and activated T lymphocytes (7–10). There is increased local production of OPN in human rheumatoid joints, and it is expressed in invading synoviocytes, chondrocytes, and CD4+ synovial T cells (2,4,11,12).

OPN contains an RGD site that mediates its attachment to osteoclast $\alpha v\beta 3$ integrin and a CD44-binding domain for bone matrix interaction, both of which are involved in bone resorption (13). In addition to $\alpha v\beta 3$, the RGD site can interact with multiple other integrins, including $\alpha v\beta 1$, $\alpha v\beta 5$, $\alpha 5\beta 1$, and $\alpha 8\beta 1$, conferring on OPN many cytokine-like functions, such as chemotaxis and signal transduction (5,6). Notably, OPN has a conserved thrombin cleavage site at ^{168}RS^{169} that is immediately downstream of the ^{159}RGD^{161} site. Thrombin cleavage exposes a new carboxyl-terminus (^{162}SVVYGLR^{168}) in the cleaved OPN (resulting in OPN-R) that interacts with $\alpha 4\beta 1$ and $\alpha 9\beta 1$ integrins in a non-RGD–dependent manner (14–19). Both integrin $\alpha 4\beta 1$ (expressed on lymphocytes and smooth muscle cells) and integrin $\alpha 9\beta 1$ (expressed on neutrophils, epithelial cells, and smooth muscle cells) represent a defined subset within the broad integrin family. The essential role of SVVYGLR in OPN in a murine model of RA has been recently reported (3). A monoclonal antibody directed against this site inhibits proliferation of synovium, infiltration of inflammatory cells, and development of bone erosions in vivo. The presence of cleaved OPN fragments has been detected in the synovial fluid of RA patients, although the precise fragments were not defined (12).

We have previously demonstrated that thrombin-activatable procarboxypeptidase B (pCPB; also called thrombin-activatable fibrinolysis inhibitor), upon activation to CPB, cleaves the C-terminal arginine from SVVYGLR, thereby converting OPN-R to OPN- L, and inhibits the enhanced OPN-R adhesion to Jurkat cells (20). Prothrombin fragment F_{1+2} and thrombin–antithrombin complexes, both indices of thrombin generation, are found at much higher levels in RA synovial fluid than in RA plasma (21), suggesting that there is a prothrombotic environment within the inflammatory joint compartment that is capable of generating thrombin locally for hydrolysis of OPN. Thrombomodulin, an essential cofactor for the activation of pCPB to CPB by thrombin and normally present on the vascular endothelial cell surface, is also present on synovial lining cells (22). Both soluble thrombomodulin (22) and pCPB (21) are greatly increased in RA synovial fluid. OPN cleavage by thrombin is dependent on both of the anion-binding exosites in thrombin that determine rates and specificity of thrombin proteolysis, establishing OPN as a physiologic substrate for thrombin (23).

To further investigate the importance of OPN-R and OPN-L in vivo, we developed specific enzyme-linked immunosorbent assays (ELISAs) for these cleaved OPN forms. We demonstrated that elevated levels of OPN-R and OPN-L are present in the synovial fluid of RA patients, and that OPN-R and OPN-L differentially regulate synoviocyte adhesion and neutrophil survival, two cellular responses known to play central roles in the pathogenesis of RA.

MATERIALS AND METHODS

Reagents. Rabbit polyclonal antibodies were raised against the peptides SVVYGL (anti–OPN-L), SLAYGLR (anti–OPN-R), and VDTYDRGDSVVYGLR (anti-OPN) conjugated to keyhole limpet hemocyanin according to a previously established standard protocol (Covance, Denver, PA). Antibodies cross-reactive with OPN-L in anti–OPN-R were removed by adsorption on Sepharose-linked SLAYGL. The human OPN Quantikine ELISA kit, anti-human OPN monoclonal antibody (mAb14331), goat anti-human OPN antibody (AF1433), and purified recombinant eukaryotic human and mouse OPN were purchased from R&D Systems (Minneapolis, MN). Anti-OPN antibody 10A16 was purchased from IBL-America (Minneapolis, MN). Peroxidase- or fluorescein isothiocyanate (FITC)–conjugated goat anti-rabbit antibody, FITC-conjugated donkey anti-mouse antibody, and Cy3-conjugated goat anti-mouse IgG antibody were purchased from Jackson ImmunoResearch (West Grove, PA). An Amino-Link Plus Immobilization kit was purchased from Pierce (Rockford, IL). Human thrombin and pCPB were purchased from Haematologic Technologies (Essex Junction, VT). The Actichrome CPB Activity kit and antithrombomodulin and anti-pCPB monoclonal antibodies were purchased from American Diagnostica (Stamford, CT). Potato carboxypeptidase inhibitor (CPI) and all other reagents and chemicals, unless stated otherwise, were purchased from Sigma (Atlanta, GA). OPN peptides were synthesized at the peptide synthesis facility at Beckman Center, Stanford University School of Medicine. High protein–binding 96-well ELISA plates were purchased from Greiner Bio-One (Monroe, NC).

Preparation of OPN-R and OPN-L from human milk–derived OPN and recombinant OPN. Full-length human milk OPN (23,24) or recombinant human OPN (OPN-FL) (both at 10 μg), quantitated by extinction at 280 nm, were digested with 100 n*M* thrombin (for OPN-R) or with thrombin followed by 100 n*M* CPB (for OPN-L) in 20 m*M* HEPES (pH 7.6), 1 m*M* $CaCl_2$, 150 m*M* NaCl, 0.1% polyethylene glycol 8000. Thrombin was quenched with PPACK (5 μM); no further treatment of CPB was required due to its thermal instability. OPN-R and OPN-L were used without further purification.

Development of specific ELISAs for human OPN-R and OPN-L. A commercially available antibody (mAb14331; 500 ng/well) was used for the capture of OPN-FL, OPN-R, and

OPN-L. OPN-FL was measured using the Quantikine OPN ELISA kit. Captured OPN-R and OPN-L were detected with anti–OPN-R or anti–OPN-L in conjunction with peroxidase-conjugated goat anti-rabbit antibody and tetramethylbenzidine substrate (Alpha Diagnostic, San Antonio, TX). Recombinant OPN-FL, OPN-R, and OPN-L (0.023–1.5 n*M*, 0.625–50 ng/ml) were used to construct the calibration curves.

Epitope mapping of anti–OPN-R and anti–OPN-L antibodies. The sandwich ELISA system using milk-derived OPN-R or OPN-L (10 ng/ml) was used for epitope mapping. Molar excesses of the ratio of peptides to antibody (50-fold) were preincubated for 2 hours and then added to the wells. Peptides SAAYGLR, SLGYGLR, SLAAGLR, SLAYALR, SLAYGAR, SLAYGLA, SLAYGLR-NH2, and RLGYALS were incubated with anti–OPN-R antibody, and SAVYGL, SVAYGL, SVVAGL, SVVYAL, SVVYGA, SVVYGL-NH2, and RLGYALS were incubated with anti–OPN-L antibody (substituted residues are underlined). The decrease in binding of the antibody to the immobilized OPN-R or OPN-L by the cognate unsubstituted peptide was defined as 100% inhibition, to which results from the substituted peptides were normalized.

Detection of OPN-FL and its cleaved forms in the synovial fluid of RA, osteoarthritis (OA), and psoriatic arthritis (PsA) patients. Synovial fluid specimens were obtained from 26 RA, 18 OA, and 10 PsA patients according to human subject protocols at Stanford University Medical Center and Brigham and Women's Hospital, and were stored frozen at −80°C until the time of analysis. Samples were thawed on ice, and clarified by centrifugation at 400*g* for 10 minutes at 4°C. The various forms of OPN were measured using the specific ELISAs. Wilcoxon's rank sum test was performed to assess the significance of difference between patient groups, and *P* values less than 0.05 were considered significant.

Multiplex cytokine analysis of synovial fluid. A 12-cytokine Beadlyte kit (Millipore, Billerica, MA) and an xMAP 100IS platform (Luminex, Austin, TX) were used to analyze synovial fluid samples. To block nonspecific crosslinking by rheumatoid factor, samples were preincubated with 3 μg/ml HeteroBlock (Omega Biologicals, Bozeman, MT). Wilcoxon's rank sum test was used to compare the median cytokine levels in samples from RA patients with levels in samples from OA patients. The correlation between cytokine and OPN levels was determined using Spearman's correlation analysis ($\rho < 0.01$ for all reported values).

Immunofluorescence labeling of fibroblast-like synoviocytes (FLS). FLS obtained from human synovial fluid samples were cultured in Dulbecco's modified Eagle's medium with 10% fetal bovine serum (FBS). Cells at passages 6–8 were used in immunofluorescence studies performed according to standard procedures.

Reverse transcriptase–polymerase chain reaction (RT-PCR) for pCPB detection in FLS. Total RNA (~1 μg) prepared from FLS was converted to complementary DNA using an oligo(dT) primer and Superscript II (Invitrogen, Carlsbad, CA). The specific primers used for amplifying a 454-bp pCPB fragment were CGTTTCAGAGTGGCCAAGTT (forward) and GGCATTTTTGGCTGTTTGTT (reverse). Annealing temperature used in the PCR was 55°C for 35 cycles.

Activation of pCPB by thrombin in the presence of cultured FLS. The functional activity of thrombomodulin on the surface of FLS was determined by adding pCPB (40 n*M*) and thrombin (10 n*M*) to phosphate buffered saline (100 μl) and incubating at room temperature for 30 minutes. The reactions were stopped with PPACK (10 μM). CPB activity was assessed using a chromogenic assay (Actichrome CPB kit). CPI (10 μg/ml) was added to inhibit CPB activity in some assays.

Direct ELISA for pCPB, OPN-R, and OPN-L. Synoviocytes were cultured in a 96-well plate and washed, and agonists were added at 37°C for 30 minutes. Aliquots of supernatants were transferred to a new 96-well plate and coated at room temperature for 2 hours. Nonspecific binding sites were blocked by incubation with bovine serum albumin (BSA; 2%) for 1 hour, followed by anti-pCPB, anti–OPN-R, or anti–OPN-L antibodies for 1 hour, and then developed in the OPN ELISAs as described above.

Immunohistochemical detection of OPN-FL and OPN-R in RA synovium. Synovial tissue samples were obtained from RA patients during total knee replacement surgery. Patients provided informed consent, and procedures followed human subject protocols approved by Stanford University Medical Center. Tissue specimens were snap-frozen and then embedded. For immunofluorescence analyses, cryosections were stained with anti–OPN-R or preimmune rabbit IgG. All cryosections were costained with anti-OPN monoclonal antibody (10A16). FITC-conjugated goat anti-rabbit IgG antibody was used to detect anti–OPN-R staining, and Cy3-conjugated goat anti-mouse IgG antibody was used to detect 10A16 staining. Some cryosections were preincubated with thrombin (100 n*M*) for 30 minutes before fixation to generate OPN-R in situ. Peptide quenching was performed by preincubation of anti–OPN-R with the peptide SLAYGLR in a 100 to 1 peptide to antibody molar ratio for 1.5 hours. Hematoxylin and eosin staining was performed according to standard procedures.

Neutrophil apoptosis assay. Neutrophils were isolated from buffy coat cells at the Stanford Blood Center using density gradient Ficoll separation, washed with RPMI 1640 with 10% FBS, and seeded into a 24-well plate at a density of 10^6 cells/ml. Cells were incubated with various concentrations of recombinant wild-type (WT) and RGD-mutated human OPN-FL, OPN-R, and OPN-L for 22 hours at 37°C in the presence of 5% CO_2. Cells were then washed and labeled with annexin–FITC and propidium iodide using an Apoptosis Assay Kit II (BD Biosciences, San Jose, CA), and analyzed by fluorescence-activated cell sorting.

Adhesion assay for FLS to OPN-FL, OPN-R, and OPN-L. Recombinant WT and RAA-substituted OPN-FL, OPN-R, and OPN-L (100 n*M*), as well as RGDS, GRGES, SVVYGLR, and SVVYGL peptides (0.1–1,000 μM), were coated onto 96-well micro black fluorescence plates (Thermo Scientific, Waltham, MA). The recombinant proteins were prepared as described previously (20). Wells were washed and blocked using 2% BSA for 1 hour. FLS were labeled with CFDA cell tracer dye, (Invitrogen) and 5,000 cells/well were incubated for 1 hour at 37°C. The wells were washed, and fluorescence was read (excitation and emission wavelengths $\lambda_{ex488\ nm}$ and $\lambda_{em538\ nm}$, respectively) using Fluoroskan Ascent (Thermo Scientific); data were recorded as relative fluorescence units.

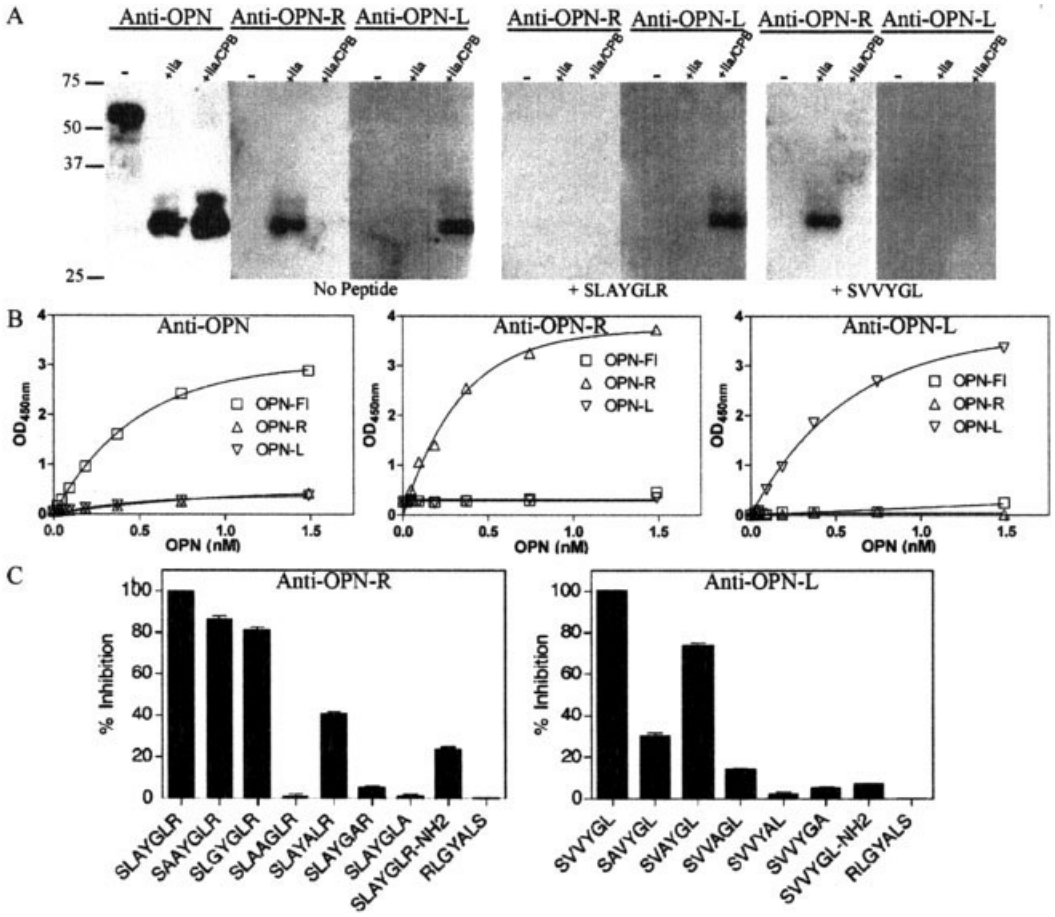

Figure 1. Characterization of specific antibodies against full-length osteopontin (OPN-FL), OPN-R, and OPN-L, and the development of specific enzyme-linked immunosorbent assays (ELISAs). Recombinant human OPN-FL was digested with thrombin (IIa) or thrombin plus carboxypeptidase B (CPB) to produce OPN-R and OPN-L, respectively. **A,** Western blot analysis of human OPN-FL, OPN-R, and OPN-L with the specific antipeptide antibodies anti-OPN, anti–OPN-R, and anti–OPN-L. OPN-R (SLAYGLR) and OPN-L (SVVYGL) peptides were used to determine competitive inhibition of antibody binding. **B,** Detection of OPN-FL, OPN-R, and OPN-L by ELISA. Values are the mean. **C,** Competition of substituted peptides for binding of anti–OPN-R and anti–OPN-L to immobilized purified OPN-R and OPN-L, respectively. Inhibition of binding by the cognate unsubstituted peptide was defined as 100%. Values are the mean and SEM. OD = optical density.

RESULTS

Generation and characterization of specific antibodies for OPN-R and OPN-L. Testing of purified rabbit IgG for various forms of OPN was completed using Western blot analysis (Figure 1A). Anti-OPN antibodies (raised against VDTYDRGDSVVYGLR) recognized all 3 forms of human OPN (OPN-L, OPN-R, and OPN-FL), and anti–OPN-R antibodies (raised against the mouse sequence SLAYGLR) recognized both mouse and human OPN-R. After removal of antibodies that were cross-reactive with OPN-L from anti–OPN-R using adsorption on Sepharose-linked SLAYGL, the immunoadsorbed anti–OPN-R was then specific for both human and mouse OPN-R. The anti–OPN-L antibodies (raised against the human sequence SVVYGL) recognized human OPN-L specifically. The specificity of the antibodies was confirmed using blocking peptides. The peptide SLAYGLR blocked the interaction of anti–OPN-R with either human or mouse OPN-R but had no effect on anti–OPN-L recognition of human OPN-L (Figure 1A). Conversely, the peptides SVVYGL (Figure 1A) and SLAYGL (results not shown) blocked anti–OPN-L recognition of human OPN-L, but had no effect on anti–OPN-R recognition of OPN-R.

Development of ELISAs specific for OPN-R and OPN-L. Anti–OPN-R and anti–OPN-L antibodies were used to develop ELISAs specific for human OPN-R and OPN-L, respectively. Purified recombinant human OPN

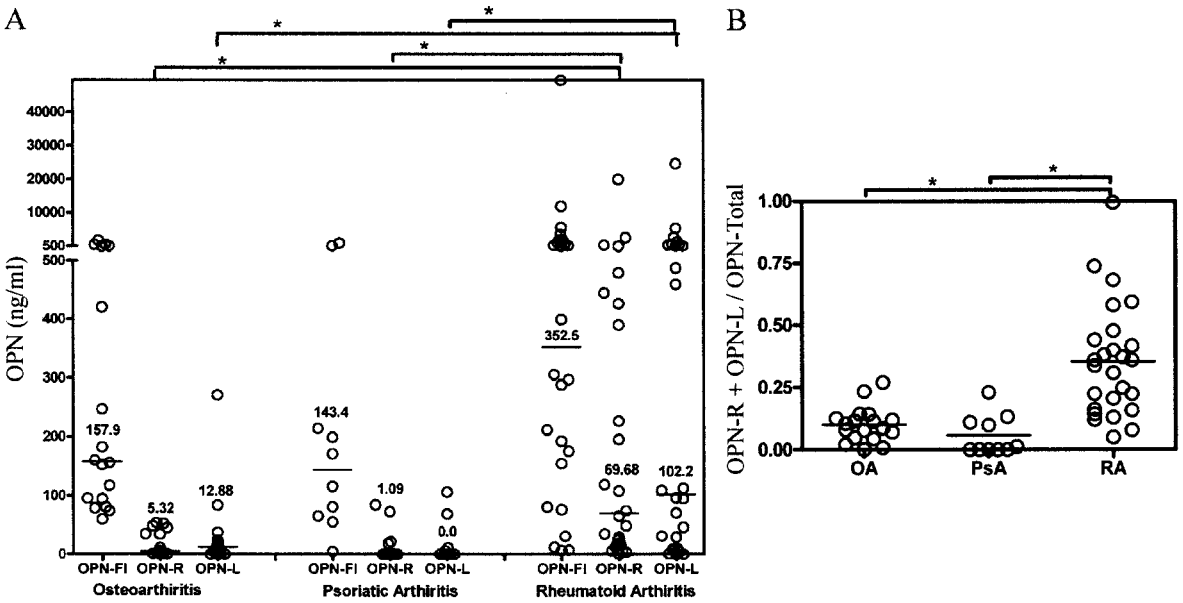

Figure 2. Levels of full-length osteopontin (OPN-FL), OPN-R, and OPN-L in the synovial fluid of patients with osteoarthritis (OA; n = 18), psoriatic arthritis (PsA; n = 10), and rheumatoid arthritis (RA; n = 26). **A,** OPN-FL, OPN-R, and OPN-L levels determined using enzyme-linked immunosorbent assay. Horizontal lines with numbers show the median. $* = P < 0.003$, by Wilcoxon's rank sum test. **B,** The ratio of cleaved OPN levels (OPN-R plus OPN-L) to total OPN (sum of the 3 OPN forms) in OA, PsA, and RA patients. Horizontal lines show the median. $* = P < 0.003$.

was cleaved with thrombin to produce OPN-R and then further cleaved with CPB to produce OPN-L, which were then used to construct the calibration curves for the ELISAs. A commercially available monoclonal antibody (mAb14331) that recognizes all 3 forms of human OPN was used as the capturing antibody in these ELISAs. With the commercially available Quantikine ELISA kit, all 3 forms of OPN could be detected, but sensitivity was much greater for detecting OPN-FL than for detecting either OPN-R or OPN-L (Figure 1B). When anti–OPN-R was used as the detecting antibody, OPN-R, but not OPN-FL or OPN-L, was detected in a dose-dependent manner, with a lower limit of detection of 0.023 n*M* (0.625 ng/ml) (Figure 1B). Likewise, anti–OPN-L specifically recognized OPN-L and not OPN-FL or OPN-R, with similar sensitivity (Figure 1B). A 20-fold molar excess in the ratios of either OPN-FL to OPN-R or OPN-FL to OPN-L did not affect the results of either of the ELISAs (data not shown), indicating that these 2 ELISAs are effective in measuring OPN-R and OPN-L levels in biologic fluid samples. As a further illustration of the specificity of the ELISAs, we found that soluble human OPN-R peptide (SVVYGLR) competitively inhibited the measurement of OPN-R, whereas OPN-L peptide (SVVYGL) did not, while soluble OPN-L peptide inhibited OPN-L measurement, whereas OPN-R peptide did not (data not shown).

To define the epitopes in OPN-R and OPN-L recognized by the respective antibodies, a series of peptides based on mouse OPN-R (SLAYGLR) and human OPN-L (SVVYGL) carboxyl-terminus sequences were synthesized and used to competitively inhibit antibody binding to immobilized OPN-R and OPN-L in the ELISA. Peptides that had key residues substituted were unable to compete effectively. For recognition by either antibody, the C-terminal arginine or leucine and its carboxyl group, as well as the adjacent amino acid, were critical (Figure 1C). In addition, anti–OPN-R antibody recognition depended on tyrosine, while the anti–OPN-L antibody recognition depended on glycine, tyrosine, and N-terminal valine.

Determination of OPN-FL, OPN-R, and OPN-L levels in the synovial fluid of patients with RA, OA, and PsA. Increased OPN levels in RA synovial fluid samples have been reported previously (4,12). We tested whether OPN-R and OPN-L were detectable in RA synovial fluid, using our specific ELISAs. While OPN-FL levels were significantly elevated in synovial fluid samples from RA patients (median 352.5 ng/ml; n = 26) compared with normal plasma levels (~50 ng/ml), OPN-FL levels

Table 1. Inflammatory cytokine levels in the synovial fluid of the RA and OA patients*

	RA patients (n = 26)	OA patients (n = 13)	P†	OPN-FL	OPN-R	OPN-L
FGF-2, pg/ml	66.6 (51.2–124.8)	15.0 (8.6–37.5)	<0.001	–	0.463	0.485
IP-10, μg/ml	19.2 (14.9–20.0)	11.5 (8.1–12.7)	<0.001	–	0.446	–
IL-12p40, pg/ml	158.0 (19.2–235.3)	0 (0–35.6)	0.001	–	0.619	0.54
IL-6, pg/ml	2,375.0 (999.5–3,502.5)	253.0 (27.5–2,185.0)	0.003	0.676	0.524	0.437
TNFα, pg/ml	81.6 (49.3–151.75)	17.2 (14.4–17.2)	0.005	–	0.434	–
Eotaxin, pg/ml	165.0 (88.1–388.5)	0 (0–147.5)	0.02	–	–	0.469
GM-CSF, pg/ml	14.0 (3.8–54.6)	0 (0–16.4)	0.05	–	–	–
MCP-1, pg/ml	174.0 (70.1–517.0)	209.0 (50.0–393.0)	0.697	–	–	–

* Values for cytokine levels in the rheumatoid arthritis (RA) and osteoarthritis (OA) patients are the median (interquartile range). Values for full-length osteopontin (OPN-FL), OPN-R, and OPN-L are correlations with the inflammatory cytokine levels, by Spearman's rank correlation, using data from all synovial fluid samples. Spearman's rho values from significant correlations ($P < 0.01$) are shown. FGF-2 = fibroblast growth factor 2; IP-10 = interferon-γ–inducible 10-kd protein; IL-12p40 = interleukin-12p40; TNFα = tumor necrosis factor α; GM-CSF = granulocyte–macrophage colony-stimulating factor; MCP-1 = monocyte chemotactic protein 1.
† By Wilcoxon's rank sum test.

in RA synovial fluid samples were not significantly elevated compared with levels in the samples from patients with OA (median 157.9 ng/ml; n = 18) ($P = 0.142$) or PsA (median 143.4 ng/ml; n = 10) ($P = 0.074$) (Figure 2A). In contrast, a highly significant elevation of OPN-R and OPN-L levels was detected in RA synovial fluid samples compared with levels in OA and PsA samples. The median values of OPN-R in RA, OA, and PsA synovial fluid were 69.7 ng/ml, 5.3 ng/ml, and 1.1 ng/ml, respectively ($P < 0.003$, for RA versus the other 2 groups), and the median values of OPN-L in RA, OA, and PsA synovial fluid were 102.2 ng/ml, 12.9 ng/ml, and an undetectable amount, respectively ($P < 0.006$, for RA versus the other 2 groups). The intact and cleaved OPN levels in the synovial fluid samples from RA patients ranged from an undetectable amount to >50,000 ng/ml, suggesting significant disease heterogeneity. The median value for the ratio of cleaved OPN (OPN-R plus OPN-L) to total OPN was ~0.35 (Figure 2B), indicating extensive enzymatic cleavage activity within the RA inflammatory joint space, whereas in samples from OA patients it was ~0.1, suggesting much less proteolytic activity.

Cytokine levels in RA and OA synovial fluid. Bead array multiplex cytokine analysis was performed in synovial fluid samples from patients with RA (n = 26) and OA (n = 13). In RA synovial fluid, levels of the proinflammatory cytokines tumor necrosis factor α (TNFα), fibroblast growth factor (FGF), granulocyte–macrophage colony-stimulating factor (GM-CSF), interferon-γ–inducible 10-kd protein (IP-10), interleukin-12p40 (IL-12p40), IL-6, and eotaxin were significantly increased (Table 1) and all, except for GM-CSF, were correlated with OPN-FL, OPN-R, or OPN-L. Notably, while increased OPN-FL levels were significantly correlated only with IL-6, increased OPN-R levels were significantly correlated with IL-6, IL-12p40, FGF-2, IP-10, and TNFα. Findings were similar for OPN-L levels, which were significantly correlated with FGF-2, IL-12p40, IL-6, and eotaxin.

Production of pCPB by RA and OA synoviocytes, release into synovial fluid, and activation by thrombin in the presence of synovial thrombomodulin. An ~65-kD protein similar to plasma pCPB was identified in RA and OA synovial tissue lysates by Western blot analysis (Figure 3A). A similar protein in cultured FLS lysates from RA and OA patients was also observed (results not shown). The anti-pCPB antibody also strongly labeled the cytoplasm of FLS (Figure 3B). RT-PCR with specific primers for pCPB revealed the expected 454-bp amplification product using FLS RNA, the identity of which was confirmed by direct sequencing. Western blot analysis also revealed pCPB in the synovial fluid of RA and OA patients (results not shown). Collectively, the data indicate that FLS synthesize and release pCPB into synovial fluid. Functional assays demonstrated CPB activity in synovial fluid from OA patients (median 2.2 μg/ml; n = 8) and RA patients (median 4.56 μg/ml; n = 9) ($P < 0.05$). The presence of thrombomodulin in FLS was demonstrated by immunofluorescence, consistent with previously published data (22) (Figure 3B). When pCPB was added to cultured FLS in the presence of thrombin, significant levels of CPB activity were generated, which was subsequently inhibited when antithrombomodulin antibody was added (Figure 3C), indicating that synovial FLS express functional thrombomodulin that can support thrombin activation of pCPB.

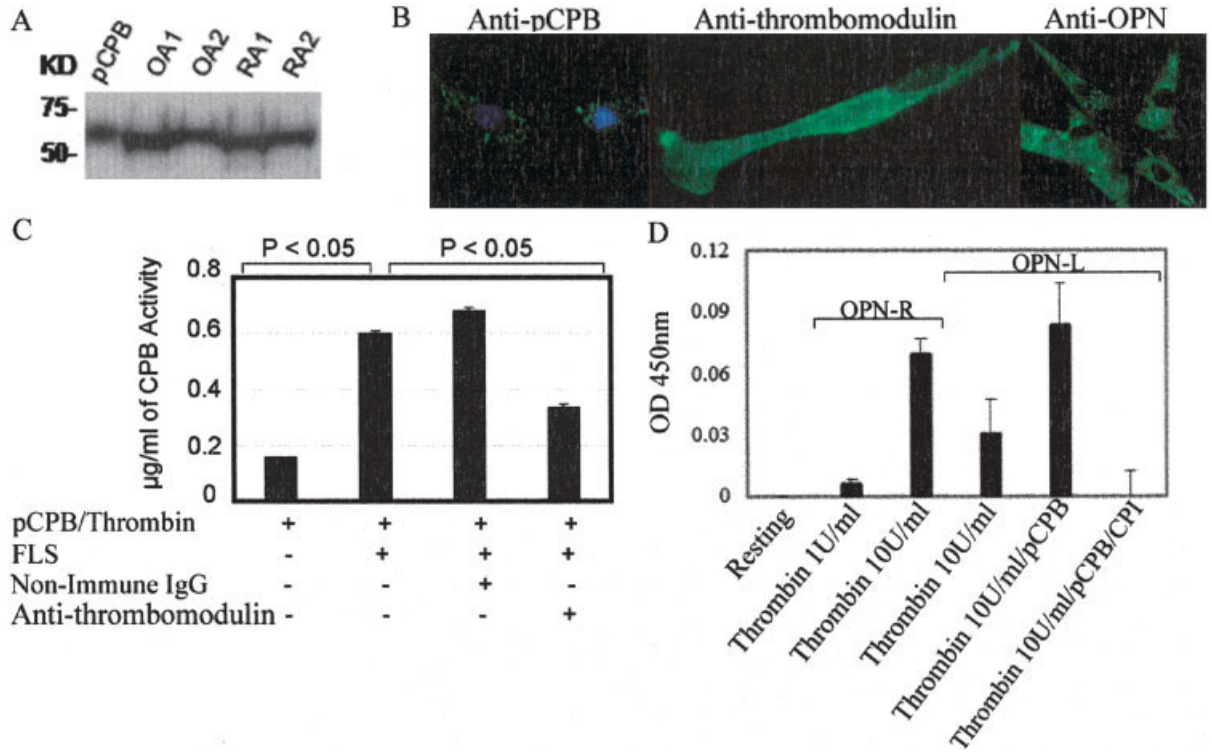

Figure 3. Identification of thrombin-activatable procarboxypeptidase B (pCPB) and its activity in fibroblast-like synoviocytes (FLS). **A,** Detection of pCPB in the synovial tissue lysates of 2 osteoarthritis (OA) patients and 2 rheumatoid arthritis (RA) patients, by Western blot analysis using an anti-pCPB monoclonal antibody. **B,** Immunofluorescence cell labeling of pCPB, thrombomodulin, and OPN in FLS. In the anti-pCPB panel, the green color indicates pCPB, and the blue color indicates nuclear labeling with 4′,6-diamidino-2-phenylindole. **C,** Enhancement of activation of thrombin-activated pCPB by thrombomodulin expressed on FLS. Activation of pCPB was blocked in the presence of antithrombomodulin antibody. Values are the mean and SEM (n = 6). **D,** Generation of endogenous OPN-R and OPN-L by incubation of thrombin with FLS, with or without exogenous pCPB. Thrombin was used at either 1 unit/ml or 10 units/ml; OPN-R ($P < 0.05$, for thrombin 10 units/ml versus resting) or OPN-L ($P < 0.05$, for thrombin 10 units/ml/pCPB versus resting, thrombin 10 units/ml, or thrombin 10 units/ml/pCPB/potato carboxypeptidase inhibitor [CPI]) in FLS supernatant was measured by direct enzyme-linked immunosorbent assay. CPI is a specific inhibitor of CPB. Values are the mean and SEM (n = 6). $P < 0.05$. OD = optical density.

Generation of OPN-R and OPN-L by thrombin and pCPB in the presence of FLS. By immunofluorescence, cultured FLS were strongly stained with anti-OPN monoclonal antibody (Figure 3B), confirming increased local production of OPN in RA synovial tissue (12). When thrombin was added to the FLS, generation of OPN-R in the supernatant was observed (Figure 3D), demonstrating thrombin cleavage of the endogenously produced OPN. Notably, OPN-L was also detectable in the supernatant (Figure 3D), indicating that thrombin, in the presence of FLS-expressed thrombomodulin, was capable of activating the endogenous pCPB into active CPB and converting OPN-R to OPN-L in vitro. The OPN-L concentration was further enhanced by the addition of exogenous pCPB, and the carboxypeptidase activity was completely abolished by potato CPI, a specific CPB inhibitor, indicating that the carboxypeptidase activity was derived from CPB and not carboxypeptidase N.

Detection of OPN-FL but not OPN-R in RA synovium. OPN-FL was abundantly expressed in the synovial lining of RA patients (Figure 4B), whereas OPN-R was almost undetectable (Figure 4C). Thrombin treatment of synovial tissue sections (cleaving OPN-FL to OPN-R in situ) resulted in robust staining of the synovial lining with the anti–OPN-R antibody (Figure 4D) in a pattern similar to that observed for OPN-FL. This suggests that the low level of OPN-R detection in the synovial lining reflected its paucity rather than an inability of the antibody to detect OPN-R in tissue. Preincubation of the OPN-R antibody with the OPN-R peptide SLAYGLR blocked its ability to stain thrombin-treated tissue sections (results not shown), confirming its specificity. Taken together, our ELISA and immunohis-

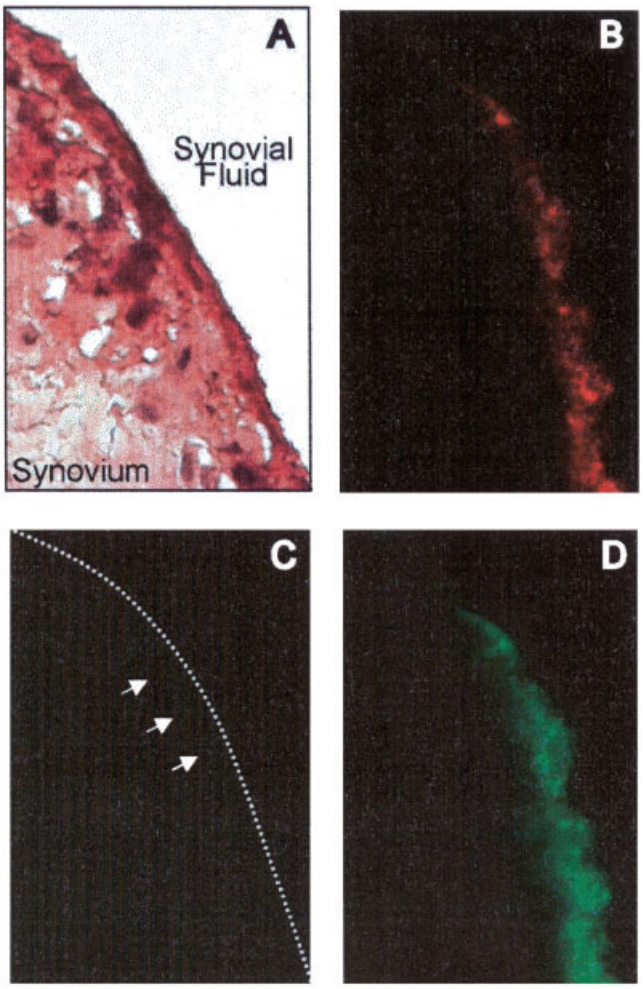

Figure 4. Detection of full-length osteopontin (OPN-FL) and OPN-R in the synovium of rheumatoid arthritis (RA) patients, by immunostaining. **A,** Hematoxylin and eosin staining. **B,** Staining with anti-OPN (10A16). **C,** Staining with anti–OPN-R. Arrows show sites of faint OPN-R staining. The stippled line represents the synovial lining. **D,** Staining with anti–OPN-R following in situ treatment with thrombin. (Magnification × 400.)

tologic data suggest that OPN-FL is highly expressed in the inflamed synovial surface, where it is cleaved by thrombin and CPB, and the cleaved OPN products are then released into the synovial fluid.

Effect of OPN and its cleaved forms on neutrophil apoptosis and cultured synoviocyte adhesion. OPN-FL, and to a lesser extent OPN-R and OPN-L, significantly protected neutrophils against apoptosis (Figure 5A). The antiapoptotic effect is dependent on the RGD site of OPN, since mutation of the RGD site in either the intact or cleaved OPN produced an almost complete loss of protection against apoptosis.

Adhesion of FLS to immobilized OPN and its cleaved forms was studied in vitro. OPN-FL increased FLS cell binding compared with BSA control (Figure 5B); this was significantly enhanced in OPN-R (>2-fold; $P < 0.05$) but not in OPN-L, suggesting that it required a functional SVVYGLR domain. Similar to the protective effect on neutrophil apoptosis, adhesion of FLS also required an intact RGD site, since mutation of the RGD site in either the intact or cleaved OPN abolished cell-binding activity. This was further demonstrated by binding of FLS to immobilized RGD but not RGE peptides and to SVVYGLR but not to SVVYGL peptides, in a dose-dependent manner (data not shown), confirming that an intact SVVYGLR domain is necessary to support the enhanced cell binding to OPN-R. FLS expressed both $\alpha 4$ and $\beta 1$ integrin subunits as confirmed by flow cytometry (data not shown), which may mediate the enhanced cell binding to OPN-R.

DISCUSSION

We have recently demonstrated that OPN is a physiologic substrate for thrombin (23). Thrombin cleavage of OPN, leading to the exposure of the cryptic $\alpha 4\beta 1$ or $\alpha 9\beta 1$ integrin–binding site in the C-terminal SVVYGLR domain in OPN-R, plays an important role in tissue inflammation (3,25–27). Our basic premise was that the subsequent cleavage of the C-terminal arginine by the thrombin/thrombomodulin-activated CPB (thereby abolishing its integrin-binding function) represents a homeostatic feedback response in modulating this inflammatory process (20). In this study, we observed the first direct evidence that thrombin-cleaved OPN-R, and thrombin- and CPB-cleaved OPN-L, are markedly elevated in the synovial fluid of RA patients (Figure 2). We performed cellular assays to investigate the roles of OPN-R and OPN-L in the pathogenesis of RA, and we describe differential regulation of FLS adhesion and neutrophil survival. The adhesion of FLS plays a critical role in the formation and growth of pannus, a tumor-like growth in the synovial lining that invades cartilage and bone and contributes to joint destruction. Neutrophils are recruited in large numbers into pannus and synovial fluid, and we demonstrate that the cleaved forms of OPN regulate neutrophil survival and apoptosis (Figure 5).

It has been well-established that thrombin has intrinsic proinflammatory properties in addition to its recognized procoagulant role in fibrin clot formation (28). Thrombin in RA may originate in part from the blood compartment, with leakage of thrombin into the

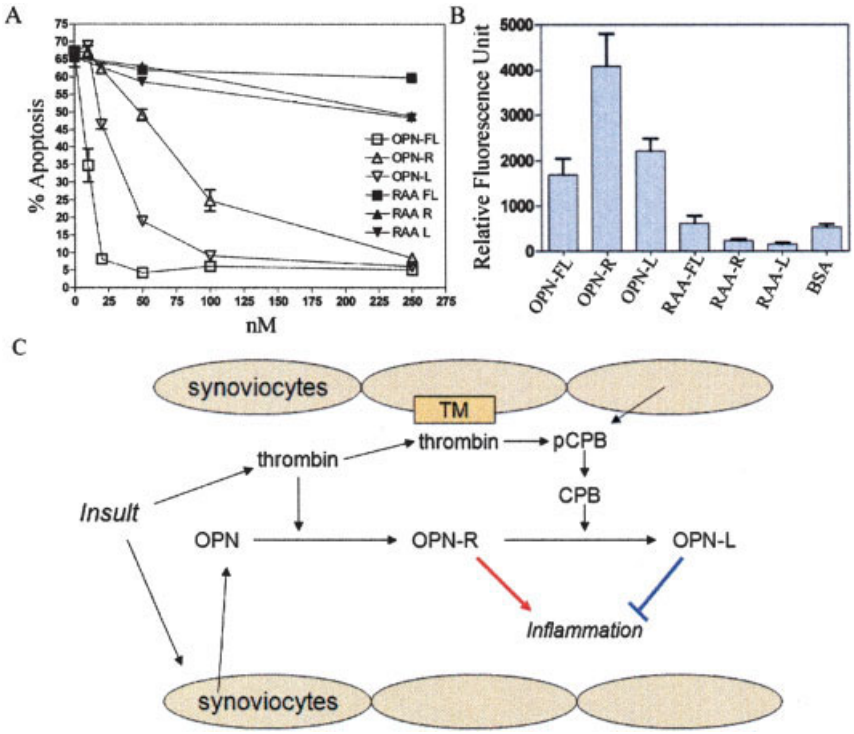

Figure 5. The effects of osteopontin (OPN) forms on neutrophil apoptosis and fibroblast-like synoviocyte (FLS) binding. **A,** Effect of recombinant wild-type (WT) full-length OPN (OPN-FL), OPN-R, OPN-L, and their RAA-substituted counterparts (RAA-FL, RAA-R, and RAA-L, respectively) on neutrophil apoptosis. Each data point represents the mean ± SEM (n = 3), and the results are representative of 1 of 3 separate experiments. **B,** FLS adhesion to immobilized WT and RGD-substituted OPN-FL, OPN-R, and OPN-L. Values are the mean and SEM (n = 8), and results are representative of 1 of 4 separate experiments. **C,** Schematic model of OPN-R and OPN-L in rheumatoid arthritis. While OPN and procarboxypeptidase B (pCPB) within the inflammatory joint space can be derived from plasma, synoviocytes also produce and release these molecules locally. Following initial insult, thrombin is generated and cleaves OPN to OPN-R, which enhances tissue inflammation. Alternatively, thrombin also binds to thrombomodulin (TM) on the synovial cell surface, which then activates pCPB locally to CPB and converts OPN-R to OPN-L, thereby dampening inflammation.

joint space a component of the inflammatory vascular response. Alternatively, thrombin may also be generated locally. Multiple clotting factors, including factor VII, factor X, and prothrombin, are present in the synovial fluid of RA patients (29,30). Thrombin-AT levels were markedly elevated in synovial fluid (50–500-fold higher levels than in plasma) (29,30). Activated neutrophils and monocytes, infiltrating the inflamed joint, are known to express tissue factor, which leads to activation of the clotting cascade and fibrin deposition locally (31). In this study, we showed that synoviocytes, in addition to their known production of OPN, synthesize and release pCPB (Figures 3A and B). Synovial cell surface thrombomodulin supports thrombin activation of pCPB to CPB, which cleaves OPN-R to OPN-L (Figures 3C and D). Thus, the whole process of synthesis and release of OPN and pCPB, thrombin activation of OPN, and its subsequent inactivation by CPB can occur within the inflamed joint space and be regulated locally (Figure 5C).

OPN confers an antiapoptotic effect on many different cell types, mediated through its binding to CD44 and/or $\alpha v\beta 3$, which may be cell-type specific (32–34). Consistent with this, OPN confers protection against apoptosis in neutrophils (Figure 5A), and it is absolutely dependent on an intact RGD site. The RAA substitution completely abolishes its antiapoptotic activity, supporting the importance of signaling through the $\alpha v\beta 3$ integrin pathway. However, it is somewhat surprising that OPN-R and OPN-L, while still quite active, have a less protective effect, since the major CD44 binding site is located at amino acids 121–140 (34) and thus, still retained within OPN-R and OPN-L. It is possible that thrombin cleavage at ^{168}R/S^{169} alters the conformation of the adjacent ^{159}RGD^{161} motif, thereby affecting its

affinity for the $\alpha v\beta 3$ integrin receptor. The enhanced synoviocyte binding to OPN-R, but not OPN-L (Figure 5B), and its direct binding to SVVYGLR, but not SVVYGL, is similar to binding via the $\alpha 4\beta 1$ receptor on synoviocytes, and is consistent with our previous observation on enhanced Jurkat cell binding to OPN-R, but not OPN-L (20). Whether OPN-R and OPN-L have distinct effects on other aspects of neutrophil and synoviocyte biology is currently being investigated.

RA is a complex disease, and a number of different pathophysiologic mechanisms could give rise to inflammatory polyarthritis that is clinically classified as RA. In this study, we observed marked heterogeneity in the elevated levels of OPN-FL, OPN-R, and OPN-L in the synovial fluid of RA patients (Figure 2). The ratio of cleaved OPN to OPN-FL (median ~0.5) suggests that in a significant subset of RA patients almost 50% of the OPN within the joint space underwent proteolytic cleavage(s). This heterogeneity may reflect different clinical severity at the time the synovial fluid samples were obtained, or intrinsic heterogeneity in the pathophysiologic mechanisms in RA. Notably, elevated levels of OPN-R and OPN-L correlated with increased levels of multiple proinflammatory cytokines including IL-6, IL-12p40, and TNFα and the chemokines IP-10 and eotaxin, while the levels of OPN-FL did not correlate with levels of proinflammatory cytokines other than IL-6 (Table 1). It is possible that elevation of OPN-FL levels is part of a general and less specific inflammatory response, and the elevated levels of OPN-R and OPN-L in a subset of RA patients suggest that thrombin- and CPB-regulated pathways may play a major role in mediating synovitis in this patient subgroup. Interestingly, hirudin, a specific thrombin inhibitor, has been shown to be efficacious in an experimental RA model (35). That finding and the results of the present study suggest that inhibition of thrombin may have therapeutic potential in these patients.

AUTHOR CONTRIBUTIONS

All authors were involved in drafting the article or revising it critically for important intellectual content, and all authors approved the final version to be published. Dr. Leung had full access to all of the data in the study and takes responsibility for the integrity of the data and the accuracy of the data analysis.

Study conception and design. Sharif, Du, Myles, Song, Nagashima, Robinson, Leung.

Acquisition of data. Sharif, Du, Myles, Song, Price, Lee, Goodman, Nagashima.

Analysis and interpretation of data. Sharif, Du, Myles, Song, Lee, Morser, Leung.

REFERENCES

1. Firestein GS. Evolving concepts of rheumatoid arthritis. Nature 2003;423:356–61.
2. Yumoto K, Ishijima M, Rittling SR, Tsuji K, Tsuchiya Y, Kon S, et al. Osteopontin deficiency protects joints against destruction in anti-type II collagen antibody-induced arthritis in mice. Proc Natl Acad Sci U S A 2002;99:4556–61.
3. Yamamoto N, Sakai F, Kon S, Morimoto J, Kimura C, Yamazaki H, et al. Essential role of the cryptic epitope SLAYGLR within osteopontin in a murine model of rheumatoid arthritis. J Clin Invest 2003;112:181–8.
4. Xu G, Nie H, Li N, Zheng W, Zhang D, Feng G, et al. Role of osteopontin in amplification and perpetuation of rheumatoid synovitis. J Clin Invest 2005;115:1060–7.
5. Denhardt DT, Noda M, O'Regan AW, Pavlin D, Berman JS. Osteopontin as a means to cope with environmental insults: regulation of inflammation, tissue remodeling, and cell survival. J Clin Invest 2001;107:1055–61.
6. Wai PY, Kuo PC. The role of osteopontin in tumor metastasis. J Surg Res 2004;121:228–41.
7. Patarca R, Saavedra RA, Cantor H. Molecular and cellular basis of genetic resistance to bacterial infection: the role of the early T-lymphocyte activation-1/osteopontin gene. Crit Rev Immunol 1993;13:225–46.
8. Ashkar S, Weber GF, Panoutsakopoulou V, Sanchirico ME, Jansson M, Zawaideh S, et al. Eta-1 (osteopontin): an early component of type-1 (cell-mediated) immunity. Science 2000;287:860–4.
9. O'Regan AW, Nau GJ, Chupp GL, Berman JS. Osteopontin (Eta-1) in cell-mediated immunity: teaching an old dog new tricks. Immunol Today 2000;21:475–8.
10. Chabas D, Baranzini SE, Mitchell D, Bernard CC, Rittling SR, Denhardt DT, et al. The influence of the proinflammatory cytokine, osteopontin, on autoimmune demyelinating disease. Science 2001;294:1731–5.
11. Petrow PK, Hummel KM, Schedel J, Franz JK, Klein CL, Muller-Ladner U, et al. Expression of osteopontin messenger RNA and protein in rheumatoid arthritis: effects of osteopontin on the release of collagenase 1 from articular chondrocytes and synovial fibroblasts. Arthritis Rheum 2000;43:1597–605.
12. Ohshima S, Yamaguchi N, Nishioka K, Mima T, Ishii T, Umeshita-Sasai M, et al. Enhanced local production of osteopontin in rheumatoid joints. J Rheumatol 2002;29:2061–7.
13. Chellaiah MA, Kizer N, Biswas R, Alvarez U, Strauss-Schoenberger J, Rifas L, et al. Osteopontin deficiency produces osteoclast dysfunction due to reduced CD44 surface expression. Mol Biol Cell 2003;14:173–89.
14. Smith LL, Giachelli CM. Structural requirements for $\alpha_9\beta_1$-mediated adhesion and migration to thrombin-cleaved osteopontin. Exp Cell Res 1998;242:351–60.
15. Taooka Y, Chen J, Yednock T, Sheppard D. The integrin $\alpha_9\beta_1$ mediates adhesion to activated endothelial cells and transendothelial neutrophil migration through interaction with vascular cell adhesion molecule-1. J Cell Biol 1999;145:413–20.
16. Yokosaki Y, Matsuura N, Sasaki T, Murakami I, Schneider H, Higashiyama S, et al. The integrin $\alpha_9\beta_1$ binds to a novel recognition sequence (SVVYGLR) in the thrombin-cleaved amino-terminal fragment of osteopontin. J Biol Chem 1999;274:36328–34.
17. Barry ST, Ludbrook SB, Murrison E, Horgan CM. Analysis of the $\alpha_4\beta_1$ integrin-osteopontin interaction. Exp Cell Res 2000;258:342–51.
18. Bayless KJ, Davis GE. Identification of dual $\alpha_4\beta_1$ integrin binding sites within a 38 amino acid domain in the N-terminal thrombin fragment of human osteopontin. J Biol Chem 2001;276:13483–9.
19. Green PM, Ludbrook SB, Miller DD, Horgan CM, Barry ST. Structural elements of the osteopontin SVVYGLR motif impor-

tant for the interaction with α_4 integrins. FEBS Lett 2001;503: 75–9.
20. Myles T, Nishimura T, Yun TH, Nagashima M, Morser J, Patterson AJ, et al. Thrombin activatable fibrinolysis inhibitor, a potential regulator of vascular inflammation. J Biol Chem 2003;278: 51059–67.
21. So AK, Varisco PA, Kemkes-Matthes B, Herkenne-Morard C, Chobaz-Peclat V, Gerster JC, et al. Arthritis is linked to local and systemic activation of coagulation and fibrinolysis pathways. J Thromb Haemost 2003;1:2510–5.
22. Conway EM, Nowakowski B. Biologically active thrombomodulin is synthesized by adherent synovial fluid cells and is elevated in synovial fluid of patients with rheumatoid arthritis. Blood 1993;81: 726–33.
23. Myles T, Leung LL. Thrombin hydrolysis of human osteopontin is dependent on thrombin anion-binding exosites. J Biol Chem 2008;283:17789–96.
24. Bayless KJ, Davis GE, Meininger GA. Isolation and biological properties of osteopontin from bovine milk. Protein Expr Purif 1997;9:309–14.
25. Diao H, Kon S, Iwabuchi K, Kimura C, Morimoto J, Ito D, et al. Osteopontin as a mediator of NKT cell function in T cell-mediated liver diseases. Immunity 2004;21:539–50.
26. Kon S, Ikesue M, Kimura C, Aoki M, Nakayama Y, Saito Y, et al. Syndecan-4 protects against osteopontin-mediated acute hepatic injury by masking functional domains of osteopontin. J Exp Med 2008;205:25–33.
27. Agnihotri R, Crawford HC, Haro H, Matrisian LM, Havrda MC, Liaw L. Osteopontin, a novel substrate for matrix metalloproteinase-3 (stromelysin-1) and matrix metalloproteinase-7 (matrilysin). J Biol Chem 2001;276:28261–7.
28. Coughlin SR. Thrombin signalling and protease-activated receptors. Nature 2000;407:258–64.
29. Carmassi F, de Negri F, Morale M, Song KY, Chung SI. Fibrin degradation in the synovial fluid of rheumatoid arthritis patients: a model for extravascular fibrinolysis. Semin Thromb Hemost 1996;22:489–96.
30. Furmaniak-Kazmierczak E, Cooke TD, Manuel R, Scudamore A, Hoogendorn H, Giles AR, et al. Studies of thrombin-induced proteoglycan release in the degradation of human and bovine cartilage. J Clin Invest 1994;94:472–80.
31. Berckmans RJ, Nieuwland R, Tak PP, Boing AN, Romijn FP, Kraan MC, et al. Cell-derived microparticles in synovial fluid from inflamed arthritic joints support coagulation exclusively via a factor VII–dependent mechanism. Arthritis Rheum 2002;46: 2857–66.
32. Burdo TH, Wood MR, Fox HS. Osteopontin prevents monocyte recirculation and apoptosis. J Leukoc Biol 2007;81:1504–11.
33. Scatena M, Almeida M, Chaisson ML, Fausto N, Nicosia RF, Giachelli CM. NF-κB mediates $\alpha v\beta 3$ integrin-induced endothelial cell survival. J Cell Biol 1998;141:1083–93.
34. Lin YH, Yang-Yen HF. The osteopontin-CD44 survival signal involves activation of the phosphatidylinositol 3-kinase/Akt signaling pathway. J Biol Chem 2001;276:46024–30.
35. Marty I, Peclat V, Kirdaite G, Salvi R, So A, Busso N. Amelioration of collagen-induced arthritis by thrombin inhibition. J Clin Invest 2001;107:631–40.